THE JOURNAL OF BIOLOGICAL CHEMISTRY VOL. 286, NO. 23, pp. 20797–20811, June 10, 2011

Amyloid β-Mediated Cell Death of Cultured Hippocampal Neurons Reveals Extensive Tau Fragmentation without Increased Full-length Tau Phosphorylation*[S]

Received for publication, February 24, 2011, and in revised form, April 7, 2011 Published, JBC Papers in Press, April 11, 2011, DOI 10.1074/jbc.M111.234674

Jack Reifert[1], **DeeAnn Hartung-Cranston**[1], **and Stuart C. Feinstein**[2]

From the Neuroscience Research Institute and Department of Molecular, Cellular, and Developmental Biology, University of California, Santa Barbara, California 93106

A variety of genetic and biochemical evidence suggests that amyloid β (Aβ) oligomers promote downstream errors in Tau action, in turn inducing neuronal dysfunction and cell death in Alzheimer and related dementias. To better understand molecular mechanisms involved in Aβ-mediated neuronal cell death, we have treated primary rat hippocampal cultures with Aβ oligomers and examined the resulting cellular changes occurring before and during the induction of cell death with a focus on altered Tau biochemistry. The most rapid neuronal responses upon Aβ administration are activation of caspase 3/7 and calpain proteases. Aβ also appears to reduce Akt and Erk1/2 kinase activities while increasing GSK3β and Cdk5 activities. Shortly thereafter, substantial Tau degradation begins, generating relatively stable Tau fragments. Only a very small fraction of full-length Tau remains intact after 4 h of Aβ treatment. In conflict with expectations based on suggested increases of GSK3β and Cdk5 activities, Aβ does not cause any major increases in phosphorylation of full-length Tau as assayed by immunoblotting one-dimensional gels with 11 independent site- and phospho-specific anti-Tau antibodies as well as by immunoblotting two-dimensional gels probed with a pan-Tau antibody. There are, however, subtle and transient increases in Tau phosphorylation at 3–4 specific sites before its degradation. Taken together, these data are consistent with the notion that Aβ-mediated neuronal cell death involves the loss of full-length Tau and/or the generation of toxic fragments but does not involve or require hyperphosphorylation of full-length Tau.

Many neurodegenerative diseases are characterized by the accumulation of aggregated proteins in the brain. For example, the microtubule-associated protein Tau forms aggregates in a variety of neurodegenerative diseases known as tauopathies, including Alzheimer, frontotemporal dementia and parkinsonism linked to chromosome 17 (FTDP-17), progressive supranuclear palsy, corticobasal degeneration, and related dementias (1, 2). Alzheimer disease is distinguished from many other tauopathies by accumulation of a second pathological feature known as amyloid β (Aβ)[3] plaques (3, 4). Complementary genetic evidence demonstrates that errors in the action or regulation of either Tau or the amyloid precursor protein (which is proteolytically cleaved to produce Aβ) can cause neuronal cell death and dementia in humans (5). Furthermore, experiments in both cultured rodent hippocampal neurons and transgenic mice demonstrate that Aβ-mediated neuronal cell death and memory deficits require Tau (6, 7). Taken together, the data suggest an intrinsic relationship between Aβ and Tau dysfunction. Indeed, the widely cited "amyloid cascade hypothesis" proposes that Aβ oligomers induce aberrant effects on Tau, which in turn promotes neurodegeneration and dementia (8–10).

One central feature of Alzheimer and related dementias is that Tau isolated from affected brains is hyperphosphorylated (11, 12). This observation led investigators to search upstream of Tau for Aβ-induced effects on the regulation of Tau-targeting kinases and phosphatases and downstream of Tau for deleterious consequences of Tau hyperphosphorylation. Unfortunately, our knowledge of the many biochemical events upstream and downstream of Tau remains poorly understood. It is known, however, that Aβ induces increased activity of several Tau-targeting kinases, including GSK3β and Cdk5 (13, 14). Additionally, hyperphosphorylated Tau has been shown to possess a reduced ability to bind and regulate microtubule behavior (15) while harboring an increased propensity to aggregate (16). Furthermore, Aβ-triggered protease activity mediates Tau fragmentation, producing potentially toxic Tau species (17, 18). A better understanding of initial Aβ-induced events and subsequent alterations to Tau as well as how these events relate to neuronal cell death is key to determining the molecular mechanisms underlying Alzheimer disease progression.

To explore the detailed molecular basis of Aβ action, with a focus on Tau dysfunction, we treated primary rat hippocampal neurons with Aβ and analyzed downstream events. Surprisingly, the data demonstrate that although GSK3β and Cdk5 appear to be activated, Aβ treatment does not dramatically affect site-specific Tau phosphorylation at any of 11 distinct

* This work was supported, in whole or in part, by National Institutes of Health Grant NS-35010. This work was also supported by the California Department of Health Services (Alzheimer's Disease Program Grant 07-65802) and the Santa Barbara Cottage Hospital Research Committee and the University of California Santa Barbara Academic Senate.

[S] The on-line version of this article (available at http://www.jbc.org) contains supplemental Figs. 1 and 2.

[1] These authors contributed equally to this work.

[2] To whom correspondence should be addressed: Neuroscience Research Institute, Bldg. 571, Rm. 6129, University of California, Santa Barbara, CA 93106. Tel.: 805-893-2659; Fax: 805-893-2659; E-mail: feinstei@lifesci.ucsb.edu.

[3] The abbreviations used are: Aβ, amyloid β; Cdk5, cyclin dependent kinase 5; GSK3β, glycogen synthase kinase 3 β; LDH, lactate dehydrogenase; Bis-Tris, 2-[bis(2-hydroxyethyl)amino]-2-(hydroxymethyl)propane-1,3-diol.

sites analyzed, including known GSK3β and Cdk5 sites, many of which are believed to be involved in pathological Tau dysfunction. In contrast, Aβ treatment does cause rapid induction of calpain and caspase 3/7 proteases, demonstrated through inhibitor pretreatments to be responsible for dramatic Tau degradation. The Aβ-induced Tau fragments are stable and appear to be phosphorylated at multiple sites. Neuronal cell death follows, which we suggest results from the combined effects of accumulated Tau fragments as well as alterations to full-length Tau. These observations have important implications for understanding the molecular basis of neuronal cell death involved in the onset and progression of Alzheimer disease.

EXPERIMENTAL PROCEDURES

Aβ Oligomer Preparation—Human $A\beta_{1-42}$ (Bachem) was solubilized and aggregated to enrich for soluble oligomers as described in Kayed *et al.* (19). Briefly, 1 mg of lyophilized Aβ peptide was resuspended in 400 μl of hexafluoroisopropanol and diluted 1:10 in sterile water. Insoluble material was removed by centrifugation at 20,000 × *g* for 10 min, and the supernatant was subjected to a gentle stream of nitrogen gas to evaporate the hexafluoroisopropanol solvent. Next, the solution was stirred at 500 rpm for 48 h at room temperature to promote oligomerization. Aggregated insoluble fibrils were subsequently removed by centrifugation for 10 min at 20,000 × *g*, and the concentration of the supernatant was determined spectrophotometrically using an extinction coefficient (ϵ_{280}) for Aβ of 1490 M^{-1} cm^{-1}, as described in Jan *et al.* (20). Generally speaking, ~75% of the starting Aβ peptide is removed as insoluble material, leaving an Aβ oligomer concentration in the soluble fraction at ~15 μM (supplemental Fig. 1). The spectrophotometric analysis was verified using a BCA colorimetric assay on the final Aβ stock solution. Aβ was added to cells immediately after the concentration determination. Both the stock solution and the resulting Aβ diluted in culture media for neuronal treatments consists of monomers and a variety of higher order Aβ oligomers (supplemental Fig. 1).

Cell Culture—Hippocampal cultures were prepared from embryonic Spraque-Dawley rats as described (21, 22). All animal work was performed in strict compliance with all applicable federal and local regulations for the proper use of animals in research. Briefly, hippocampi were dissected from E18/19 rat fetuses in Hepes-buffered Hank's balanced salt solution (Invitrogen), trypsinized (0.25%) for 10 min at 37 °C, triturated with fire-polished Pasteur pipettes, and plated at medium to high density in DMEM with 5% fetal bovine serum on poly-L-lysine-coated culture dishes (2×10^6 cells/100 mm-dish, 3×10^5 cells/well in 6-well dishes, and 1×10^4 cells/well in 96-well dishes). After 16 h, the medium was changed to Neurobasal medium supplemented with L-glutamine, 2% B-27, and 0.2% penicillin/streptomycin (Invitrogen). Subsequent half-media changes were performed every 3–4 days for 15 days, at which time Aβ treatments were initiated. This duration in culture was used because at this point cells express equal amounts of three-repeat Tau and four-repeat Tau (data not shown), which mimics the Tau isoform ratio in adult human brain (23). For immunofluorescence microscopy, hippocampal neurons were plated at low density (1×10^4 cells/well) on poly-L-lysine-coated Permanox™ 8-well chamber slides (Lab-Tek®) and cultured as described above.

Aβ Treatments—Immediately after preparation of soluble oligomers, the Aβ solution was diluted to between 0.16 and 2.5 μM in neuronal culture media derived as half-fresh media and half-conditioned media from cultures, as performed for the half-media changes described above. Neurons were exposed to Aβ for various times ranging from 1 min to 72 h. Untreated control neurons were exposed to the same volume of culture media with a mock dilution to mimic Aβ administration.

Inhibitor Treatments—Neurons were preincubated with inhibitors for 1 h before and during the duration of exposure to Aβ. The calpain inhibitor Z-L-Abu-CONH-ethyl (Calpain inhibitor X: Calbiochem) was used at 1 μM, diluted in media from a DMSO stock solution of 200 μM. The caspase inhibitor benzyloxycarbonyl-VAD-fluoromethyl ketone (Calbiochem) was used at 50 μM, diluted in media from a DMSO stock solution of 5 mM.

Cell Death Assays—After Aβ treatment for specified lengths of time, neurons were analyzed for cell death using two independent assays. The CellTiter Glo® (Promega) assay quantifies the ATP content of the primary cultures. Neurons were plated directly in 96-well dishes and treated with Aβ, and the ATP content of the cells was measured at various time points. The luminescent values were normalized between untreated control cells (100% viable) and a cell death control treatment of 200 μM staurosporine for 24 h (0% viable), which consistently gave luminescent readings only slightly above background (wells with culture media but without cells). The CytoTox-ONE™ (Promega) assay measures lactate dehydrogenase released into the culture media through compromised cell membranes (24). 100 μl of media was removed from Aβ-treated cells and placed into 96-well dishes in triplicate. The neurons were subsequently used for parallel immunoblot or microscopic analyses. LDH activity in the media was measured as per the manufacturer's protocol, and fluorescent values were normalized between untreated controls (100% viable) and Triton X lysis controls to represent the maximum amount of LDH available for release (0% viable).

Immunoblotting—Whole-cell lysates were prepared from hippocampal neurons cultured in 100 mm or 6-well dishes. An SDS-radioimmune precipitation assay lysis buffer (50 mM Tris-HCl, pH 7.6, 150 mM NaCl, 5 mM EDTA, 0.5% Triton X-100, 0.5% Nonidet P-40, 0.1% SDS, and 0.1% sodium deoxycholate) with freshly added protease (Thermo 78410) and phosphatase (Sigma P2850 and P5726) inhibitor cocktails was used for lysis. After 1 h of lysis buffer treatment at 4 °C, insoluble material was removed by centrifugation for 10 min at 20,000 × *g*, and protein concentration of the lysate was determined using a BCA assay (Thermo). Cortical tissue from adult Tau knock-out mouse brain, a kind gift from Hana Dawson (Duke University), was lysed similarly. 10–20 μg of each lysate was fractionated on 8, 12, or 4–20% SDS-PAGE gels, depending on the size of the band(s) of interest. After transferring to nitrocellulose membranes, the blots were probed with various primary antibodies listed in Table 1. When appropriate, the same blot was probed for a housekeeping protein such as GAPDH to serve as a loading control. Secondary antibodies conjugated to AlexaFluor 680

TABLE 1
List of antibodies used in this study
WB, Western blot; IFM, immunofluorescence microscopy.

	Species	Supplier	WB dilution	IFM dilution	Epitope specificity
Tau antibodies					
Tau-1	Mouse	Chemicon	1:5,000	1:500	Non-phospho-Tau at Ser-195, -198, -202, and -205
Tau-5	Mouse	BioSource	1:5,000	1:500	Phosphorylation-independent 210–230
Pan-tau	Rabbit	Laboratory-produced[a]	1:10,000	1:2,000	Total Tau protein
pTau 181	Rabbit	Millipore	1:500	1:200	Phosphorylation at Thr-181
pTau 199/202	Rabbit	Invitrogen	1:2,000	1:500	Phosphorylation at Ser-199 and -202
pTau 205	Rabbit	Millipore	1:1,000	1:500	Phosphorylation at Thr-205
pTau 217	Rabbit	Millipore	1:1,000	1:500	Phosphorylation at Thr-217
pTau 231	Rabbit	Invitrogen	1:2,000	1:1,000	Phosphorylation at Thr-231
pTau 235	Mouse	Priontype	1:5,000	1:1,000	Phosphorylation at Ser-235
pTau 262	Rabbit	Invitrogen	1:200	1:100	Phosphorylation at Ser-262
pTau 396	Rabbit	Millipore	1:2,000	1:500	Phosphorylation at Ser-396
pTau 400	Rabbit	Millipore	1:1,000	1:500	Phosphorylation at Ser-400
PHF-1	Mouse	Kind gift[b]	1:2,000	1:500	Phosphorylation at Ser-396 and 404
pTau 413	Rabbit	Santa Cruz Biotech	1:2,000	1:500	Phosphorylation at Ser-413
Signaling antibodies					
Akt	Rabbit	Cell Signaling	1:2,000	NA	Total Akt
pAkt (473)	Rabbit	Cell Signaling	1:500	NA	Akt phosphorylated at Ser-473
Erk 1/2	Mouse	Cell Signaling	1:1,000	NA	Total Erk1/2
pErk 1/2	Rabbit	Cell Signaling	1:1,000	NA	Erk 1/2 phosphorylated at Thr-202 and Tyr-204
GSK3β	Mouse	Cell Signaling	1:1,000	NA	Total GSK3β (cross-reactive to GSKα)
pGSK3β (9)	Rabbit	Cell Signaling	1:1,000	NA	Phosphorylation on GSK3β at Ser-9
p35	Mouse	Santa Cruz Biotech	1:200	NA	p35 and p25
Tubulin antibodies					
α-Tubulin (DM1A)	Mouse	Sigma	1:10,000	NA	α-Tubulin
βIII-tubulin	Mouse	Invitrogen	1:10,000	1:1,000	βIII-tubulin isoform
Acetylated tubulin	Mouse	Sigma	1:5,000	1:1,000	Acetylated α-tubulin
α-tubulin (DM1A) FITC	Mouse	Sigma	NA	1:200	α-Tubulin, FITC conjugated for microscopy
Other antibodies					
GAPDH	Mouse	Sigma	1:5,000	NA	GAPDH
Vimentin	Chicken	Millipore	1:1,000	NA	Vimentin
Spectrin	Mouse	Santa Cruz Biotechechnology	1:100	NA	αII-Spectrin (α-fordrin)

[a] From Makrides *et al.* (61) (see supplemental Fig. 2 for antibody validation).
[b] Provided by P. Davies, Feinstein Institute for Medical Research, Manhasset, NY 11030.

(1:10,000 Molecular Probes) or IRDye 800CW (1:10,000 Odyssey) were used for detection followed by imaging on a LiCor Odyssey Infrared Imager (Odyssey). Quantitation was performed using LiCor software (Odyssey), and target protein density was normalized to GAPDH internal controls.

Two-dimensional Immunoblotting—Protein was isolated from neurons using an SDS lysis buffer with freshly added protease and phosphatase inhibitor cocktails (described above) and prepared for two gels using the ReadyPrep 2-D clean-up kit (Bio-Rad). Protein concentration was determined using a BCA assay, and the lysate was diluted to 1 mg/ml. 200 μg of protein was focused isoelectrically between pH 5–8 on an 11-cm immobilized pH gradient strip using the Protean IEF Cell (Bio-Rad). The focused strips were then fractionated using 12% Criterion XT Bis-Tris precast gels (Bio-Rad). After transferring the two-dimensional separated samples to a nitrocellulose membrane, blots were probed with the primary pan-Tau antibody (Table 1, see also supplemental Fig. 2 for specificity controls). Secondary antibodies conjugated to horseradish peroxidase (1:2500, GE Healthcare) were used for protein detection with SuperSignal West Dura chemiluminescence substrate (Pierce). An EPI-Chemi Darkroom system and Labworks software (UVP Laboratory Systems) were used to image the protein blots.

Immunofluorescence Microscopy—Neurons cultured in chamber slides (described above) were fixed for 20 min with 4% paraformaldehyde in phosphate-buffered saline. Double immunolabeling was performed using pan-Tau and tubulin antibodies as indicated. For detection, tubulin antibodies directly conjugated to FITC were used (1:100, Sigma), whereas Tau antibodies were detected with either an anti-mouse Cy3 or an anti-rabbit Cy3 secondary antibody (1:200, The Jackson Labs, West Grove, PA).

Protease Activity Assays—Neurons cultured in 96-well dishes were directly measured for caspase 3/7 and calpain protease activities using substrates that upon cleavage release luminescent signals. Caspase 3/7 activity was measured using the Caspase-Glo 3/7 assay (Promega). Luminescent measurements from Aβ-treated wells (triplicate) were normalized to control, mock-treated wells (set to 1). Calpain activity was measured using the Calpain-Glo assay (Promega) and analyzed in the same fashion as the caspase assay.

Statistical Analyses—The significance of cell death and protease activity induced by Aβ treatments was analyzed by two-tailed unpaired Student's *t* test comparing treated sample data to untreated data from the same time point. Western blot densitometry data were analyzed and normalized for GAPDH housekeeping levels followed by -fold intensity comparisons between untreated and Aβ treatments for each time point. Values obtained from three independent experiments were analyzed by two-tailed unpaired Student's *t* test. Significant values are indicated and determined to have $p < 0.05$.

RESULTS

Over the past few years, a number of independent lines of evidence have converged to demonstrate that Tau is intrinsically involved in Aβ-mediated neuronal dysfunction and cell

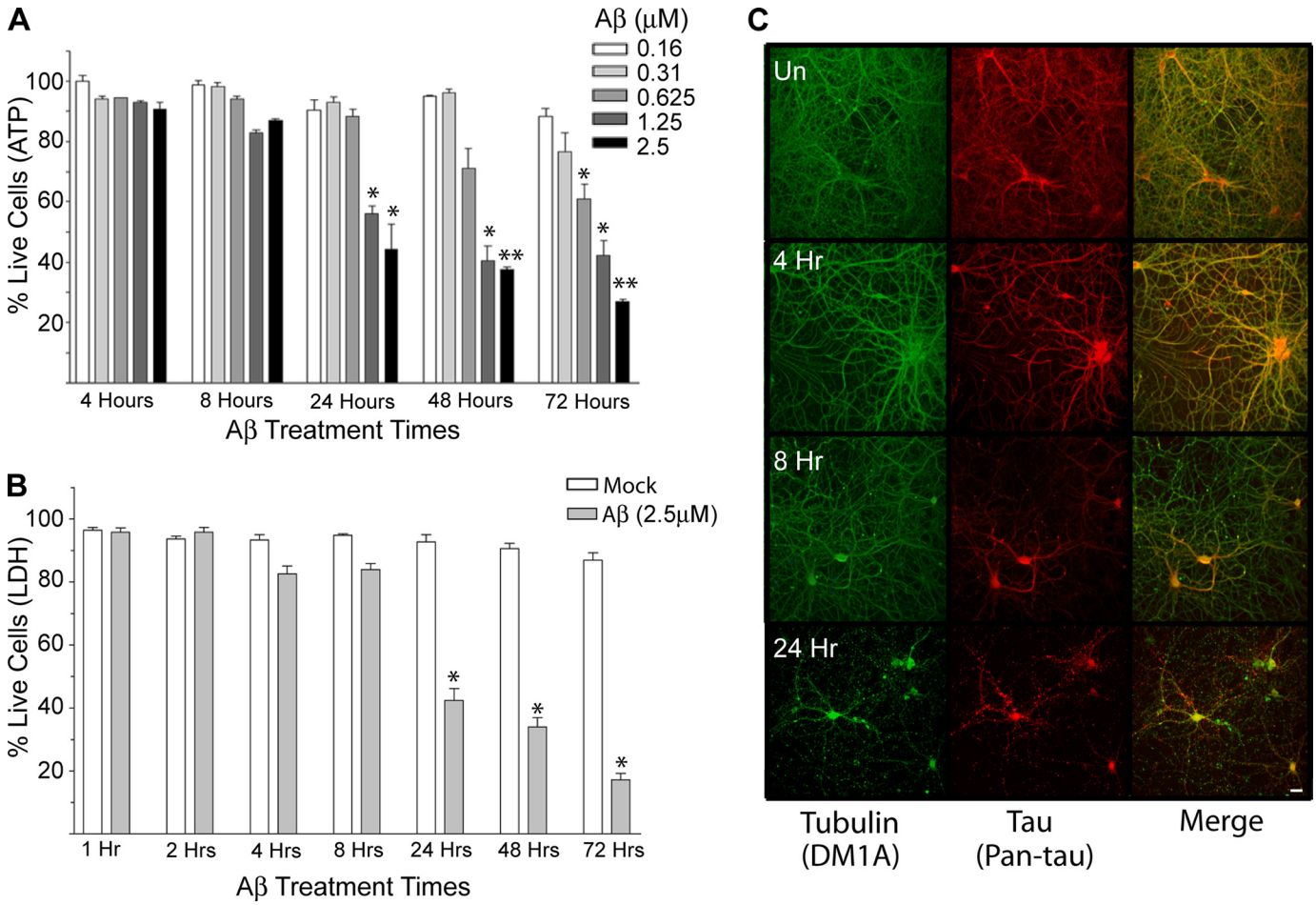

FIGURE 1. **Extensive neuronal cell death occurs between 8 and 24 h after Aβ administration.** *A*, shown is cell viability as measured by ATP content in hippocampal neuronal cultures treated with the indicated concentrations of Aβ as a function of time. 2.5 μM Aβ produces ~50% cell death after 24 h of exposure. *Error bars* represent S.E. of three independent experiments. *B*, shown is cell viability as measured by LDH released into the media when hippocampal neurons are treated with 2.5 μM Aβ for the indicated times. *Error bars* represent S.E. of at least three independent experiments. *C*, shown is immunofluorescence microscopy images of hippocampal neurons treated with 2.5 μM Aβ for the indicated times. Anti-Tau (*pan-Tau*) is *red*, and anti-α-tubulin (*DM1A*) is *green*. Magnification, 20×; *scale bar*, 10 μm. *, $p < 0.05$; **, $p < 0.01$ compared with controls. *UN*, untreated.

death (6, 7, 25, 26). The present work investigates molecular mechanisms underlying Aβ-induced cell death by identifying Aβ-mediated biochemical and cell biological effects on cultured primary neuronal cells, with an emphasis on Tau biochemistry, before, and during the period of cell death.

Significant Cell Death of Primary Rat Hippocampal Cultures Occurs between 8 and 24 h of Exposure to Soluble Aβ Oligomers—To define an appropriate time frame to analyze biochemical and cell biological changes induced by Aβ, we first determined the time-course of Aβ-mediated cell death in primary rat hippocampal neurons using two independent assays. Our initial cell death assay, measuring ATP content in cells, yielded a dose-dependent effect with Aβ treatment generating significant cell death between 8 and 24 h of exposure to 1.25–2.5 μM Aβ (Fig. 1*A*). Lower Aβ concentrations also caused cell death but required longer durations. A concentration of 2.5 μM Aβ was chosen for all subsequent analyses because of the rapidity of the response (~50% cell death in 24 h) and because this concentration is comparable with many previous cell culture studies assessing Aβ induced cell death (19, 27). Our Aβ preparation includes multiple oligomeric states (monomers, dimers, and higher order oligomers), and although it remains controversial which oligomeric state(s) contributes to toxicity, it is possible that multiple oligomer states converge in toxic function producing the rapidity and potency we observe in our assays (28, 29) (see supplemental Fig. 1 for our Aβ preparation analysis).

To confirm our time-course of Aβ-mediated neuronal cell death, we employed an independent cell death assay measuring the release of lactate dehydrogenase (24) into the media, thereby reflecting a compromised membrane structure. The pattern of LDH release in this assay was similar in kinetics and the extent to the loss of ATP in the previous cell death measurements (Figs. 1, *A* and *B*).

We next examined neuronal cell morphology at various times during a 24-h Aβ time-course using immunofluorescence microscopy to image both tubulin and Tau (Fig. 1*C*). The anti-tubulin images demonstrated that the neurons retained a relatively normal morphology for at least 8 h of exposure to Aβ. However, by 24 h, the anti-tubulin labeling revealed a beaded neuritic morphology characteristic of dead or dying neurons. The anti-Tau images presented a similar general pattern, with the exception of the 8-h time point. At this time, despite the fact that the overall neuronal morphology was largely intact, the Tau signal decreased noticeably, especially in the distal regions

of the neurites. In contrast, Tau remains readily detectable in the soma. At 24 h, the Tau signal was almost completely absent from the neurites and only remained in the cell body. Taken together, the cell death assays and imaging data both indicate that extensive neuronal cell death occurs between 8 and 24 h of exposure to 2.5 μM Aβ.

Aβ Induces Rapid Biochemical Changes in Erk1/2, Akt, GSK3β, and Cdk5 Indicative of Inactivation of Erk1/2 and Akt and Activation of GSK3β and Cdk5 Kinases—We next sought to explore the effects of Aβ treatment on neuronal cell signaling before and during the induction of cell death. Whole cell protein lysates were prepared from primary rat hippocampal neurons treated with Aβ for durations of between 3 min and 24 h. To assess relative changes in the activities of individual signaling proteins in these lysates, we immunoblotted with pairs of antibodies specific to each protein of interest. One antibody of each pair detected a phospho-epitope corresponding to the active state (or inactive state) of the signaling protein, whereas the other detected total protein independent of phosphorylation. We conducted a preliminary screen of numerous candidate signaling proteins to determine which might be affected by Aβ treatment. Most revealed little or no effect, including PTEN, ELK, RAF, DARPP32, Pin1, Bim, NFκB, and IKKα/β (data not shown). On the other hand, the preliminary screen indicated robust effects of Aβ on Erk1/2 and Akt signaling, consistent with previous work (30, 31), leading us to perform a more detailed kinetic analysis of these two signaling cascades that could be correlated with the kinetics of additional biochemical changes induced by Aβ and eventual neuronal cell death (see below).

Aβ-treated neurons demonstrated a remarkably rapid reduction in the level of Akt phosphorylation on its activation loop at serine 473, suggesting decreased Akt activity (Fig. 2*A*). Indeed, phospho-Akt decreased by 35% within only 3 min of exposure to Aβ. The reduced phospho-Akt level was maintained throughout the entire 24-h time-course, with only minor reductions in total Akt abundance late in the time-course when cell death becomes prominent. A similar, albeit perhaps slightly slower, pattern was observed for Erk1/2 (Fig. 2*B*). For both phospho-Akt and phospho-Erk1/2, signal intensity levels decreased ~6-fold after only 2 h of Aβ treatment.

Akt can regulate GSK3β activity (32), which is widely believed to regulate normal and pathological Tau activity through its ability to phosphorylate multiple sites on Tau (33). More specifically, Akt can phosphorylate GSK3β at serine 9, thereby suppressing GSK3β kinase activity (34). Therefore, we next assayed the Aβ time-course lysates for phospho-GSK3β. Phospho-GSK3β levels rapidly declined with Aβ treatment (~13-fold; Fig. 2*C*), revealing a time-course similar to or perhaps slightly slower than the phospho-Akt time-course. These data suggest rapid changes in activity levels of both kinases, consistent with a mechanism in which Aβ inactivates Akt, thereby relieving suppression of GSK3β activity.

Finally, we assessed Aβ effects upon the production of p25, an activator of Cdk5 activity, that is also widely held to regulate normal and pathological Tau activity (35, 36). Because p25 is generated via proteolytic processing of p35 (37), we indirectly assessed Cdk5 activity across the Aβ time-course by immunoblotting with an antibody recognizing both p25 and p35 and determining the relative abundance of each. Again, we observed a relatively rapid production of p25 beginning 10 min after Aβ administration and reaching maximal levels (~20-fold) after 8 h (Fig. 2*D*).

The relative signal intensities examined above are summarized in Fig. 2*E*. Taken together, these data suggest that Aβ promotes a rapid and marked decrease in Akt and Erk1/2 activities and a slightly slower but more marked increase in GSK3β and Cdk5 activities.

Aβ Induces Activation of Both Calpain and Caspase 3/7 Proteases—Calpain has been shown to cleave p35, producing p25 and thereby promoting increased Cdk5 activity (38). Because our data showed a time-dependent accumulation of p25 when neurons are treated with Aβ (Fig. 2*D*), we next sought to determine the relative activity of calpain during the Aβ time-course. Additionally, both calpain and caspase 3/7 have been implicated in generating potentially toxic Tau fragments (17, 18).

We performed calpain and caspase 3/7 activity assays on neuronal cells as a function of time in Aβ (Fig. 3). We observed a rapid induction of calpain activity, first detectable at 5 min, reaching a maximum at 10 min (a 5-fold increase) and then incrementally returning to control levels by 4 h. Caspase 3/7 activity was induced even faster but was smaller in magnitude (2-fold) and returned to control levels after only 1 h of Aβ treatment. Pretreatment of cells with calpain and caspase 3/7 inhibitors, respectively, effectively diminished the Aβ-mediated activations.

The specificities of the protease activity assays and their respective inhibitors were verified using immunoblot analysis of known substrates for calpain and caspase 3/7 present in the lysates. Aβ treatment leads to the rapid fragmentation of spectrin, producing a 150-kDa product, consistent with calpain digestion, which is effectively blocked by the calpain inhibitor (Fig. 3*C*) (39). On the other hand, spectrin cleavage is not blocked by pretreatment with the caspase 3/7 inhibitor (data not shown). These data implicate calpain as the protease responsible for spectrin cleavage and further suggest a more prominent role for calpain over caspase 3/7, as spectrin can be a substrate for both proteases (40). Additionally, Aβ treatment leads to the rapid fragmentation of vimentin (a known caspase 3/7 substrate), and this fragmentation is effectively blocked by the caspase 3/7 inhibitor (Fig. 3*D*) (41).

These data are consistent with previous observations of activated calpain and caspase proteases in Alzheimer brain (42, 43). Interestingly, our data suggest a biphasic proteolytic response to Aβ treatment in hippocampal neurons, with early caspase activation followed shortly thereafter by a larger and more sustained calpain activation.

Efficient Aβ-induced Tau Degradation Precedes the Onset of Neuronal Cell Death—Up to this point, we have investigated cellular changes induced by exposure to Aβ that may influence the onset of Tau dysfunction (*i.e.* kinase and protease activities). We next sought to examine effects of Aβ treatment on Tau itself, focusing on effects that might be mediated by proteases and kinases.

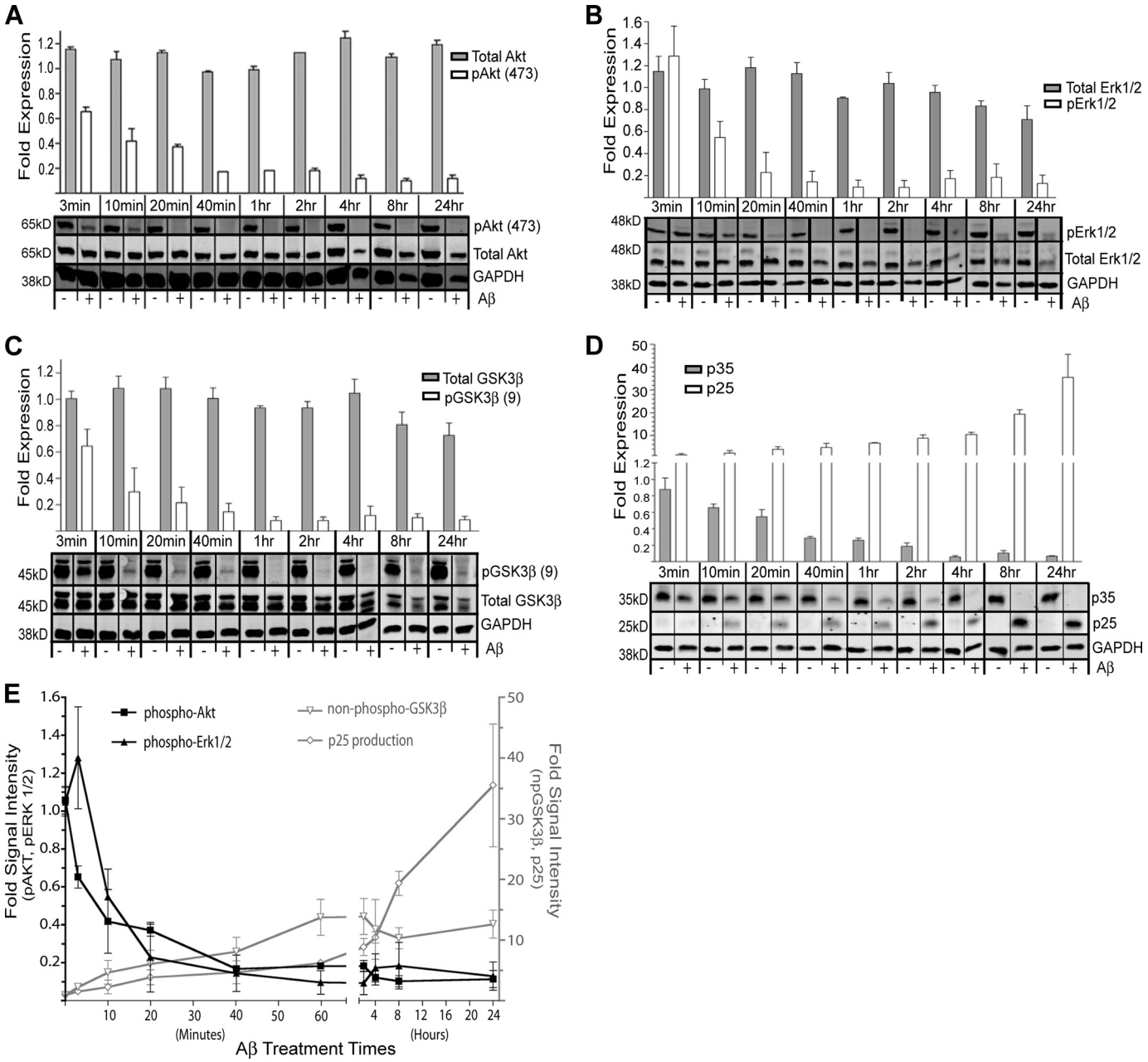

FIGURE 2. **Aβ treatment promotes biochemical changes, suggesting inactivation of Akt and Erk1/2 and activation of Tau-targeting kinases GSK3β and Cdk5.** *A*, shown are immunoblots of the survival kinase Akt and its activated form, phospho-Akt at serine 473 (*pAkt (473)*). *B*, shown are immunoblots of Erk1/2 and its activated form, phospho-Erk1/2. *C*, shown are immunoblots of GSK3β and an inactivated form, phospho-GSK3β, at serine 9 (*pGSK3β (9)*). *D*, shown are immunoblots of p35 and the production of its proteolytic fragment, p25 (an activator of Cdk5). *Panels A–D* graphically present densitometry analysis (*above*) of the respective protein levels determined by immunoblotting (*below*). For each time point we first normalize the GAPDH data from the untreated (−) and treated (+) samples. Using this correction factor, we then ratio the Aβ treated *versus* untreated signals for each band of interest to generate the -fold intensity of each treated time point (shown in the *bar graphs*). *Error bars* represent S.E. of densitometry from three independent experiments. *E*, shown is a graphic summary of the data in *A–D*. Cdk5 activity is suggested by p25 fragment production. *Non-phospho-GSK3β* (*npGSK3β*) indicates the loss of signal for phospho-GSK3β at serine 9, suggesting activation of this kinase. Kinases in *black* are graphed against the *left y axis*, whereas kinases in *gray* are graphed against the *right y axis*. Note that the *x* axis is non-linear. Error bars represent S.E. of densitometry from 3 independent experiments.

Because we observed increased caspase and calpain protease activities when neurons were treated with Aβ and these proteases have been implicated in degrading full-length Tau, we next examined the integrity of Tau during the time-course of Aβ treatment using immunoblotting analysis. We immunoblotted lysates from an Aβ time-course to assay for the presence and kinetics of Tau fragmentation (Fig. 4*A*) using a pan-Tau antibody that recognizes all Tau isoforms (see supplemental Fig. 2). In non-Aβ-treated control lysates, pan-Tau recognized three resolvable Tau bands in the size range between ~50 and 60 kDa, corresponding to intact Tau. The abundance of Tau in this region of the gel began to decline between 40–60 min into the Aβ time-course. More detailed analysis reveals the largest and least abundant of the three Tau bands disappeared very early in the time-course (within 3 min). The middle Tau band began to disappear between 20–40 min, and the smallest

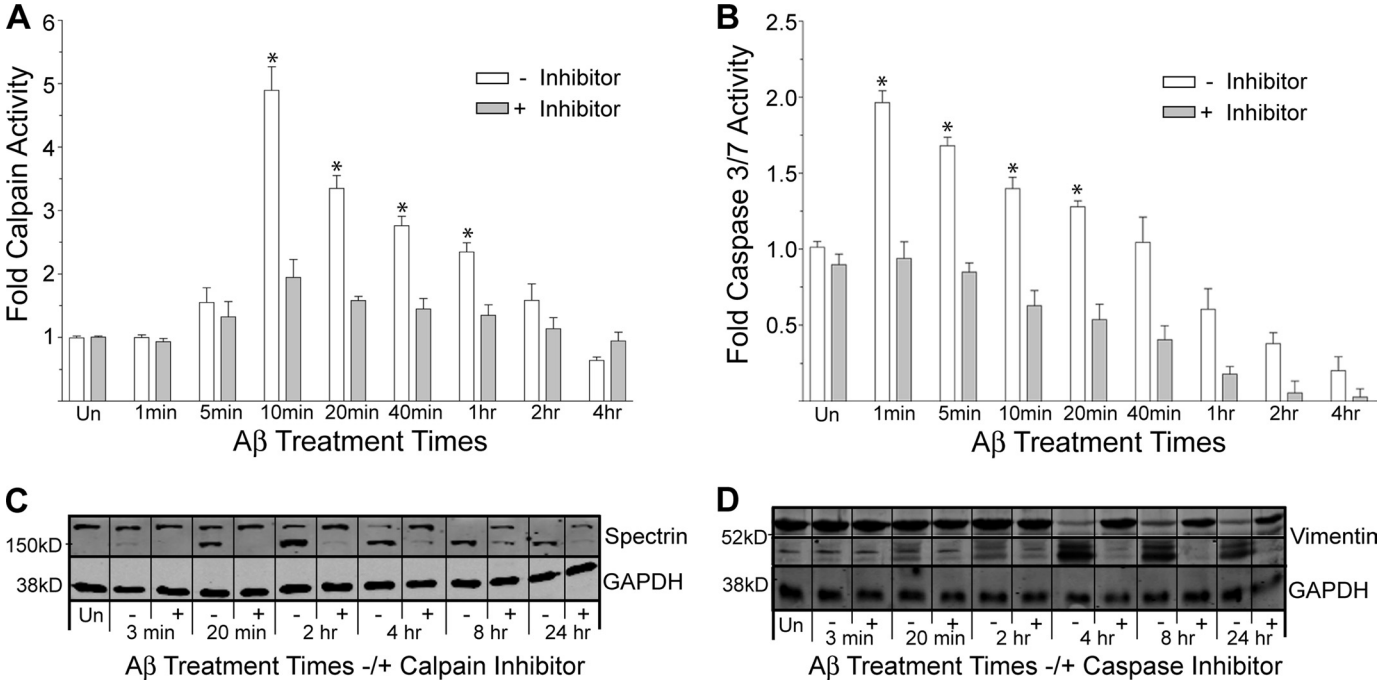

FIGURE 3. **Aβ induces rapid activation of caspase 3/7 and calpain proteases.** *A* and *B*, direct activity measurements were performed as described under "Experimental Procedures" as a function of time exposed to Aβ without (−) or with (+) the respective protease inhibitor pretreatment. Data were normalized to 1 for mock-treated controls (*Un*). *Error bars* represent the S.E. of three independent experiments. *, $p < 0.01$ compared with controls. *C* and *D*, an immunoblot analysis verifies protease activity with substrate cleavage. Calpain substrate spectrin and caspase substrate vimentin demonstrate cleavage into smaller molecular weight fragments upon Aβ treatment, both of which are protected by the respective inhibitors.

and most abundant Tau band began to disappear between 1–2 h. By 2 h, essentially no Tau migrated at the control positions, although two bands did migrate, only slightly faster. It is important to note that these slightly faster migrating species could be the result of either proteolytic cleavage of small fragments from one of the Tau ends and/or dephosphorylation, which is known to affect Tau migration on SDS/PAGE. Four hours after Aβ treatment, the vast majority of the Tau was depleted from the region of the gel corresponding to intact Tau.

When the same protein lysates were fractionated on gradient gels and probed with the Tau-5 monoclonal antibody, we observed extensive Aβ-dependent Tau fragmentation (Fig. 4*B*). After 2 h of Aβ administration, there was significant accumulation of Tau fragments with apparent molecular masses of ~24 and 17 kDa, consistent with earlier work (17). These fragments were first detectable at 10–20 min of the time-course and increased in abundance over time. Importantly, these fragments appeared to be quite stable, as the strength of their signals increased through 8 h of Aβ treatment and remained throughout the entire duration of the time-course. In fact, these fragments are still readily detectable after 72 h of Aβ treatment (data not shown). Blotting the same extracts with the Tau-1 monoclonal antibody revealed a slightly simpler fragmentation pattern but again revealed major Tau fragments at ~17 and 24 kDa without increased immunoblot exposure times as needed when probed with the pan-Tau and Tau-5 antibodies. Both Tau-5 and Tau-1 recognize epitopes in the region between amino acids 195 and 230. As controls for specificity of Tau degradation and to ensure equal protein loading, Fig. 4*A* shows a GAPDH housekeeping control immunoblot of the lysates and Fig. 4*C*, *right*, shows a Coomassie Blue-stained gel corresponding to the samples fractionated in Fig. 4*C* (44). Fig. 4*D* graphically depicts the densitometric analysis of the loss of full-length pan-Tau signal (*black line*, *left y axis*) and the accumulation of the 24- and 17-kDa fragments (*gray line*, *right y axis*) as detected by the Tau-5 antibody. Taken together, the data demonstrate that Aβ induces (i) relatively rapid and specific Tau degradation and (ii) the generation of relatively stable Tau fragments before and during the period of prominent cell death.

Protease Inhibitors Eliminate or Reduce the Production of Low MW Tau Fragments and Partially Protect Neuronal Viability upon Aβ Treatment—Calpain and caspase proteases are implicated in Tau degradation into low MW products with potential toxic function, but the contribution of each protease or both together in producing these Tau fragments and the resulting toxicity remains unclear (17, 18, 45). We, therefore, aimed to protect Tau integrity using calpain and caspase inhibitors and measured corresponding cell death induced by Aβ treatment to better understand the role Tau fragments may play in Aβ-mediated neuronal cell death.

After pretreatment for 1 h with a calpain inhibitor, a caspase inhibitor, or both together, we exposed neurons to Aβ for durations between 3 min and 72 h. Immunoblots on the prepared lysates demonstrate that both the calpain and caspase inhibitors protect against loss of full-length Tau induced by Aβ; however, the calpain inhibitor provides much more protection than the caspase inhibitor at later time points (Fig. 5*A*). Interestingly, after 4 and 8 h of Aβ treatment, the pan-Tau immunoblots revealed the retention of full-length Tau when calpain was inhibited and to a lesser degree with caspase inhibition compared with Aβ treatment alone, but neither inhibitor (or inhibition of both proteases together) protected against the pro-

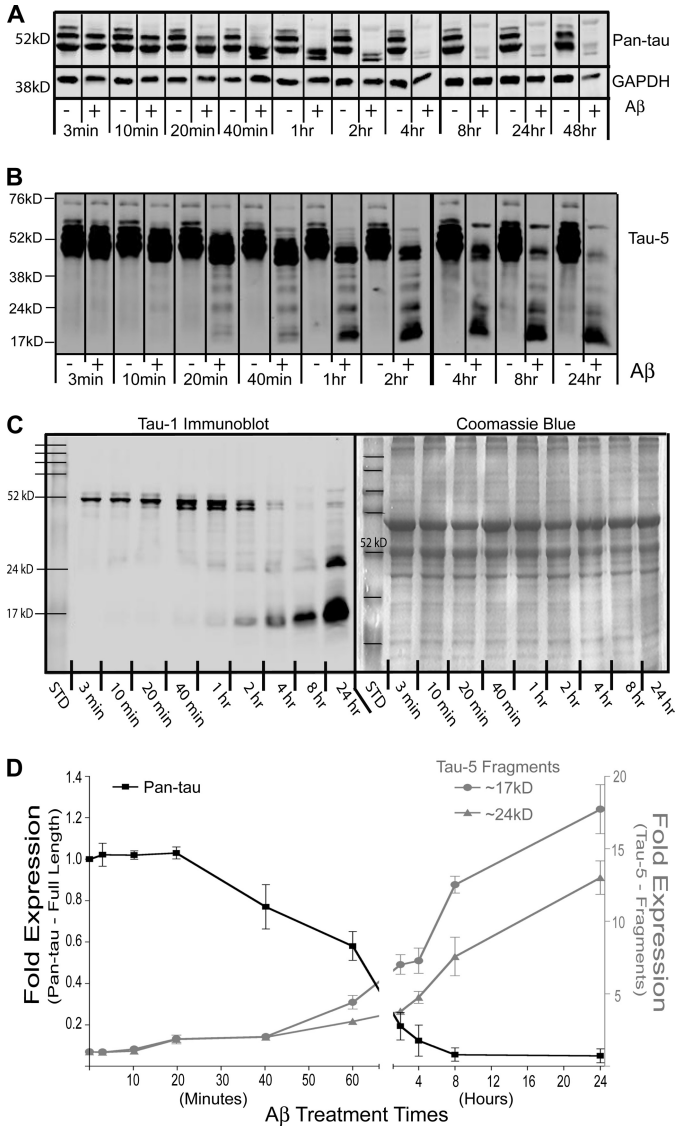

FIGURE 4. **Aβ induces rapid Tau degradation and the production of relatively stable low molecular weight fragments.** *A*, full-length Tau immunoblots were detected using the pan-Tau antibody. The GAPDH housekeeping signal is shown *below*. *B*, Tau-5 immunoblot highlights the fragmentation pattern and accumulation of low molecular weight Tau fragments. *C*, the Tau-1 blot corroborates the generation of low molecular weight Tau fragments along with a Coomassie Blue stained gel, demonstrating protein integrity and lack of general degradation. The *line graph* shown in *D* presents the loss of full-length Tau as a function of time exposed to Aβ (graphed against the *left y axis*) and the production of the 24- and 17-kDa Tau fragments (graphed against the *right y axis*). Note that the *x axis* is non-linear.

duction of the slightly faster-migrating Tau bands produced at early time points of Aβ treatment. The production of the 24- and 17-kDa Tau fragments upon Aβ treatment is completely abolished when calpain is inhibited and partially abolished when caspase is inhibited, demonstrating a differential protective response with each of the inhibitors (Fig. 5*B*). Inhibition of both proteases together is only as protective as the calpain inhibitor alone, further suggesting a more prominent calpain activation (compared with caspase activation) upon Aβ treatment.

Given that the calpain and caspase 3/7 inductions precede the onset of Aβ-mediated neuronal cell death, we next asked if these induced proteolytic activities contributed to Aβ-mediated neuronal cell death by conducting a dose-response analysis of Aβ treatment in the presence or absence of protease inhibitors. When neuronal cell death was measured between 24 and 72 h of 2.5 μM Aβ exposure using the ATP assay, a moderate protection was observed with the calpain inhibitor, whereas only a minimal protection was observed with the caspase inhibitor pretreatment (Fig. 5*C* and data not shown). This result prompted us to explore a dose titration of Aβ to determine whether the protease inhibitors might provide more dramatic protection at lower Aβ concentrations. As seen in Fig. 5*C*, the calpain inhibitor but not the caspase 3/7 inhibitor provided protection against loss of ATP at all concentrations tested. This is especially apparent in the linear parts of the curves on either side of the 1 μM points. We also performed a time-course analysis of Aβ-mediated neuronal cell death using the LDH assay, holding the Aβ concentration at 2.5 μM. In this analysis both inhibitors provided considerable protection against cell death, with the calpain inhibitor providing somewhat more protection than the caspase 3/7 inhibitor. Importantly, as was true in the ATP content assay, neither inhibitor provided complete protection (Fig. 5, *C* and *D*). In fact, cell death was still observed even when both inhibitors were present simultaneously. Although it is unclear exactly why the two different cell death assays yielded somewhat different results, we suspect that the ATP assay is more sensitive to early metabolic alterations in the cell death pathway, whereas the LDH release assay corresponds to late-stage cellular destruction. We conclude that both calpain and caspase 3/7 contribute to Aβ-mediated neuronal cell death, with calpain playing a greater role.

Neurons Treated with Aβ Exhibit Only Transient and Limited Increases in Tau Phosphorylation—Thus far we have demonstrated a time-course of elevated caspase and calpain proteolytic activities leading to Tau fragmentation, which precedes neuronal cell death. Because our data also suggest rapid increases in GSK3β and Cdk5 kinase activities upon Aβ exposure, we next sought to define the kinetics of site-specific effects of Aβ upon Tau phosphorylation. Based on the literature (for review, see Ref. 46) and our kinase activity data, we expected to observe marked and widespread increases in Tau phosphorylation in Aβ-treated neurons relative to non-Aβ-treated control cells. We selected 11 different phosphorylation sites for analysis (amino acid positions 181, 199/202, 205, 217, 231, 235, 262, 396, 400, 396/404, 413) based in large part upon literature citations implicating particular Tau sites in Alzheimer pathology (46). Surprisingly, there were no sustained increases in phosphorylation at any of these sites (Fig. 6, *A* and *B*). Four sites exhibited modest transient increases in phosphorylation upon Aβ exposure, which then decreased below their corresponding control levels within very short periods of time. More specifically, positions 205 and 262 exhibited clear and significant increases in phosphorylation after only 3 min of exposure to Aβ, with levels returning to those of controls by 10 min. Phosphorylation at amino acid position 400 exhibited a more sustained increase in signal, returning to its control level within 1 h. Phosphorylation at amino acid position 181 also showed a subtle but sustained increase between 3 min and 1 h of Aβ exposure; however, this trend was not statistically significant. Several controls were

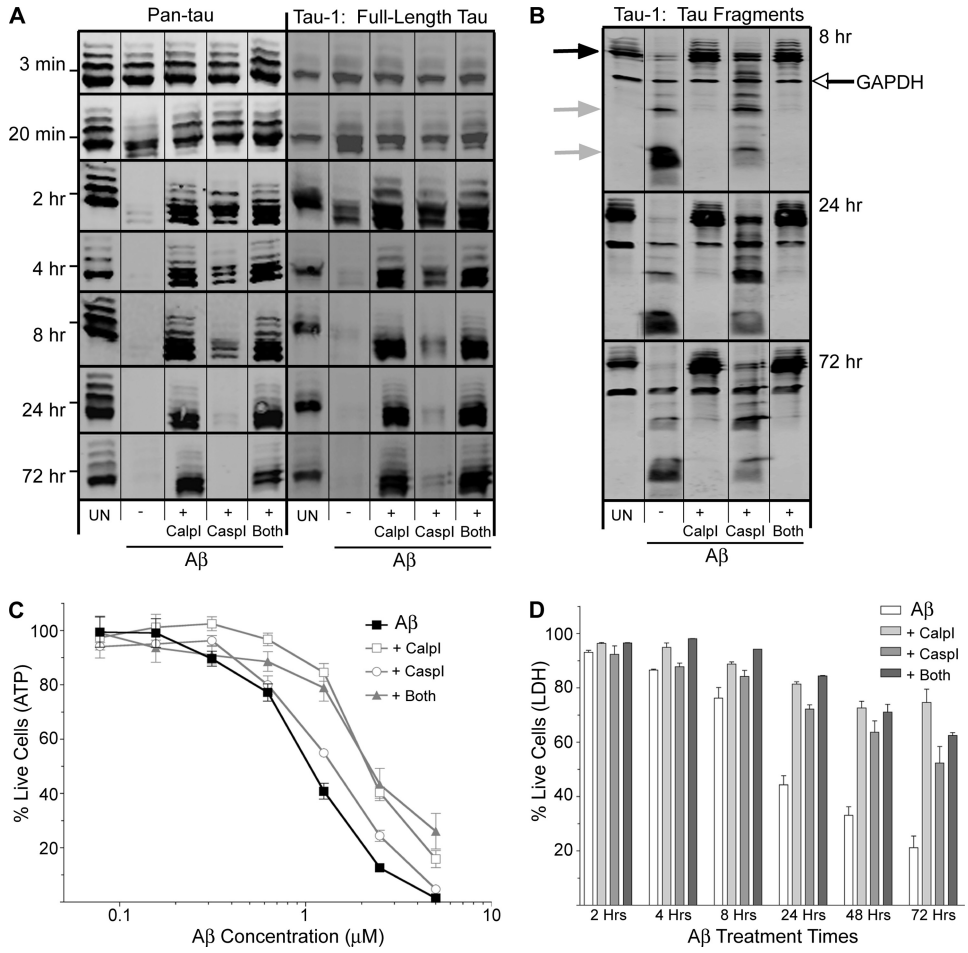

FIGURE 5. **Calpain and caspase protease inhibitors differentially protect against Tau degradation as well as Aβ-mediated cell death.** *A*, Pan-Tau and Tau-1 immunoblots after Aβ treatment between 3 min and 72 h. *Marks to the left* of the immunoblots indicate the 53-kDa size standard. *B*, Tau-1 immunoblots 8, 24, and 72 h after Aβ treatment show Tau fragmentation into 24- and 17-kDa products (*gray arrows*). Full-length Tau (*black arrow*) and GAPDH signals (*open arrow*) are indicated. *C*, cell viability was measured by ATP content after 72 h of treatment of a dose titration of Aβ. The *graph* is representative of data from two independent experiments. *Error bars* represent S.E. of replicate wells. *D*, cell viability was measured by LDH release after treatment with 2.5 μM Aβ for the indicated times. *Error bars* represent S.E. from at least two independent experiments. *A–D*, *UN*, untreated samples; *Aβ −*, Aβ without any inhibitor treatment; *Aβ + CalpI*, Aβ with calpain inhibitor treatment; *Aβ + CaspI*, Aβ with caspase inhibitor treatment; *Aβ + Both*, Aβ with both calpain and caspase inhibitor treatment.

employed for these assays. First, to assess the Tau specificity of the various antibodies, we assayed cortical extracts from an adult Tau knock-out mouse (a kind gift from Hana Dawson). With the exception of antibodies directed against phospho Tau 231 and 235, none of the site- and phospho-specific Tau antibodies recognized any proteins in the lysates, demonstrating their specificities. Anti-phospho Tau 231 and anti-phospho Tau 235 detected high molecular weight bands in the Tau knock-out mouse extract, well above any Tau band in the normal rat extracts. It is likely that these bands correspond to MAP2, which is a relatively large protein that shares extensive sequence homology with Tau. Second, multiple loading controls were used, including GAPDH, α-tubulin, and βIII-tubulin.

Because Aβ-mediated Tau degradation is rapid and we cannot rule out that the lack of detection of Tau phosphorylation was due to rapid loss of full-length Tau, we also probed lysates pretreated with the calpain inhibitor followed by Aβ exposure, suspecting that protection against Tau degradation may expose epitopes on Tau that become phosphorylated. Surprisingly, although Tau is readily detectable with the pan-Tau, Tau-1, and Tau-5 antibodies with calpain inhibition throughout the time-course, none of the phospho-specific antibodies demonstrated long-term increases in signal intensity. In fact, only three antibodies (phospho-Tau 231, 400, and 413) detected Tau in the Aβ + calpain inhibitor lysates after 2 h of Aβ exposure, and these gave only low intensity signals (data not shown).

Another important observation is that, with the possible exception of anti-phospho Tau 235, none of the other phospho-specific antibodies detected any of the Tau proteolytic fragments (data not shown) that are detected by pan-Tau, Tau-5, and Tau-1 antibodies (Fig. 4, *C* and *D*).

Along with the phospho-Tau analysis, we also examined a tubulin post-translational modification: acetylation. Interestingly, Aβ treatment induced a rapid and sustained increase in tubulin acetylation, which returned to non-Aβ-treated levels at 8 h in the Aβ time-course. A recent report indicates that tubulin acetylation combined with removal of Tau from the axon may increase the sensitivity of the microtubules to be cleaved by katenin (47), suggesting a possible mechanism for axonal degradation upon Aβ treatment.

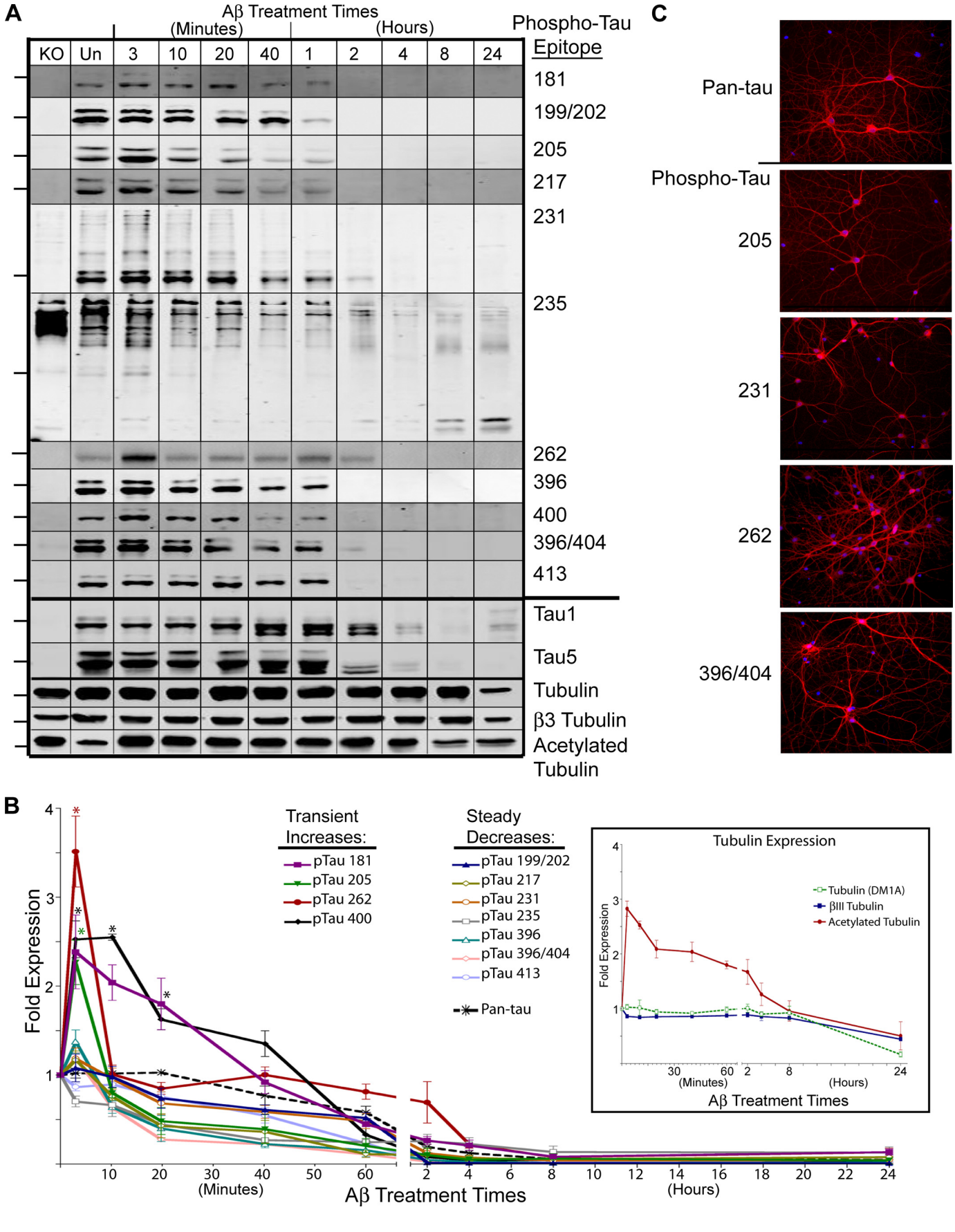
A
Aβ Treatment Times
(Minutes)
(Hours)
KO
Un
3
10
20
40
1
2
4
8
24
Phospho-Tau Epitope
181
199/202
205
217
231
235
262
396
400
396/404
413
Tau1
Tau5
Tubulin
β3 Tubulin
Acetylated Tubulin
C
Pan-tau
Phospho-Tau
205
231
262
396/404
B
Transient Increases:
pTau 181
pTau 205
pTau 262
pTau 400
Steady Decreases:
pTau 199/202
pTau 217
pTau 231
pTau 235
pTau 396
pTau 396/404
pTau 413
Pan-tau
Fold Expression
(Minutes)
(Hours)
Aβ Treatment Times
Tubulin Expression
Tubulin (DM1A)
βIII Tubulin
Acetylated Tubulin

Finally, we also examined the localization of each phospho-Tau epitope by immunofluorescence microscopy. As examples, Fig. 6*C* shows untreated, control cultures stained with four different phospho-Tau antibodies. In all cases, staining was observed primarily in neurites but also in somas to a lesser extent. The remaining seven phospho-specific antibodies generated similar images to those shown. These data demonstrate that healthy neurons express basal levels of Tau phosphorylated at each of these specific sites and that this observed level of phosphorylation is not inherently toxic. Parallel images were also captured for each phospho-Tau antibody during the time-course of Aβ treatment with no observable differences relative to the pan-Tau images shown in Fig. 1 (data not shown).

In summary, the most important observation among these data was the very surprising lack of dramatic effects of Aβ treatment upon site-specific Tau phosphorylation. However, it should be noted that the transient increases observed in specific phosphorylated epitopes could mediate important structural and/or regulatory effects on Tau biochemistry that may influence subsequent cellular events.

Two-dimensional Immunoblotting Demonstrates the Lack of a General Aβ-mediated Effect on Full-length Tau Phosphorylation—The unexpected absence of a dramatic and widespread Aβ effect on site-specific Tau phosphorylation led us to question if we might have missed the bulk of a major phosphorylation effect by assaying Tau phosphorylation in a site-specific manner. Therefore, we fractionated lysates from the Aβ time-course using two-dimensional gels and probed the immunoblots with the pan-Tau antibody. Because the first dimension is isoelectric focusing and each phosphorylation event adds negative charges to its substrate, a marked effect on Tau phosphorylation at any site (including those not assayed above) would appear as a shift in Tau migration toward the acidic side of the gel. For frame of reference, based on the amino acid sequence of rat Tau, a Tau molecule possessing two phosphates has a predicted pI of 6.96, and a Tau molecule possessing 6 phosphates has a predicted pI of 6.25 (calculation at Scansite at the Massachusetts Institute of Technology). Preliminary experiments demonstrated that the different species of Tau with different isoelectric points separate optimally between a pI of 5 and 8. This result is consistent with reports that the pIs of recombinant Tau isoforms range from 7.1 to 8.5, whereas Tau isolated from Alzheimer brain can have isoelectric points as low as 5 (48, 49). We fractionated lysates from neurons treated with Aβ for up to 4 h. As seen in the Sypro Ruby stain of fractionated non-Aβ treated extract (Fig. 7, *top left*), our gels effectively resolve the proteins in the extract. Pan-Tau immunoblotting of a non-Aβ-treated lysate (*Un panel*) showed that the most prominent Tau species were detected between a pI of 7 and 8 at the full-length size. Lighter exposures reveal many individual spots at different sizes and charges (data not shown). At the 20-min Aβ time point and to a lesser extent at the 3-min time point, a small subset of Tau became acidified (note the *arrows* in Fig. 7). Importantly, the observed acidification was transient and did not persist beyond the 20-min time point. By 40 min in the time-course, the full-length Tau signal looked much like the non-Aβ-treated sample. Thus, this general assay for Aβ-mediated acidification of Tau did not detect the shift in isoelectric point that would be predicted if Aβ-induced a dramatic increase in Tau phosphorylation at sites other than those assayed in Fig. 6.

On the other hand, consistent with the one-dimensional gel analyses in Fig. 4, the two-dimensional gels detected extensive Aβ-mediated Tau fragmentation as early as 20 min in the time-course. Interestingly, these low molecular weight fragments exhibited a broad range of pIs. The periodicity of the Tau fragments migrating in the isoelectric focusing dimension (most obvious in the 4-h time point) suggests that these Tau fragments likely vary from one another by virtue of numbers of phosphates per fragment, which is especially interesting because we did not detect any significant amount of Tau fragment phosphorylation with any of the 11 site-specific antibodies (data not shown). This leads to the conclusion that these fragments are likely phosphorylated on some subset of the remaining ~20 known Tau phosphorylation sites. Fig. 8 summarizes the kinetics of the events we observed when treating hippocampal neurons with Aβ oligomers.

DISCUSSION

To develop effective therapeutics for Alzheimer and related dementias, it is essential that we acquire a thorough understanding of the biochemical events contributing to neuronal cell death in these diseases. Toward that goal, this work sought to define a detailed kinetic timeline of biochemical events in a well controlled neuronal cell culture system. We began with administration of Aβ oligomers and ended with the induction of neuronal cell death, focusing on candidate signaling pathways altered by Aβ and a detailed analysis of Tau fragmentation and Tau phosphorylation. The most important findings were as follows. 1) Aβ oligomers rapidly induce robust calpain and caspase proteolytic activities, with activity measurements and substrate cleavage data, both, suggesting calpain activation is more prominent than activation of caspase 3/7. 2) Aβ oligomers rapidly reduce levels of phospho-GSK3β while promoting the cleavage of p35 into p25, suggesting increased activity of both GSK3β and Cdk5. 3. Tau degradation is first detected after only 10–20 min of Aβ administration. By 2–4 h, very little full-length Tau remains, and there is a substantial accumulation of a series of relatively stable Tau fragments. Inhibitor studies indicate that Tau fragmentation is largely mediated by calpain and, to a lesser extent, caspase 3/7. 4) Surprisingly, Aβ administration does not dramatically increase full-length Tau

FIGURE 6. **Aβ does not induce sustained increases in Tau phosphorylation at 11 single or double epitopes analyzed.** *A*, shown are immunoblots of Aβ-treated hippocampal neuronal lysates probed for 11 different phospho and site-specific Tau antibodies as well as Tau-1, Tau-5 and tubulin antibodies. *Marks to the left* of the immunoblots indicate the 53-kDa size standard. *KO*, lysates from Tau knock-out mouse brain. *Un*, untreated samples. *B*, shown is quantitative analysis of the phospho-Tau immunoblots in *A*, with untreated samples for each time-course set to 1. The *inset graph* displays analysis for total, βIII, and acetylated tubulin immunoblots. *Error bars* represent S.E. for three independent experiments. *, $p < 0.05$ compared with untreated control. *C*, immunofluorescence microscopy of untreated neurons stained for pan-Tau and the phospho-Tau antibodies indicated is shown. The Tau stain is *red*, whereas the nuclear stain is *blue*. Magnification, 20×.

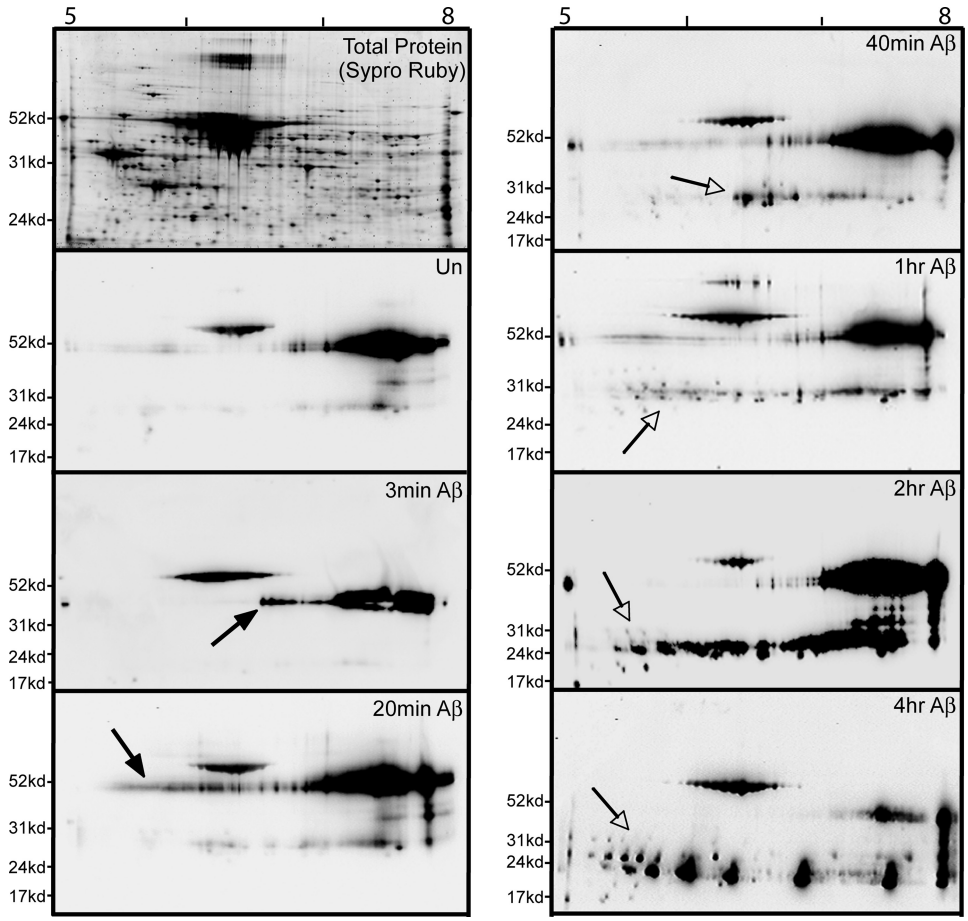

FIGURE 7. **Two-dimensional immunoblotting demonstrates that Aβ treatment does not induce sustained acidic shifts in Tau isoelectric points as would be predicted from hyperphosphorylation.** Shown are two-dimensional anti-Tau immunoblots (using anti-pan-Tau) on a time-course of Aβ-treated neuronal lysates first separated by pI between 5 and 8 and then separated by molecular weight. At the *top left* is a Sypro Ruby-stained gel of a control neuronal cell lysate, demonstrating good separation and resolution of total cellular proteins. An untreated (*Un*) blot defines the two-dimensional pattern of control Tau. Additional blots correspond to the designated time in the presence of Aβ. *Solid arrows* point to a small subset of Tau exhibiting an acidic pI shift at 3- and 20-min time points; however, this signal is no longer present at later times. *Open arrows* point to the prominent accumulation of low molecular weight Tau fragments starting after 40 min of Aβ treatment and accumulating through 4 h of treatment.

phosphorylation, as assayed by immunoblots with 11 different site- and phospho-specific antibodies as well as two-dimensional immunoblotting using a pan-Tau antibody. However, subtle and transient increases in Tau phosphorylation are observed at 4 distinct sites on Tau, at positions 181, 205, 262, and 400. 5) Stable fragments of Tau induced by Aβ administration are likely to become phosphorylated, as suggested by their altered isoelectric points on two-dimensional gels.

Consistent with previous work by Park and Ferreira (17) and Gamblin *et al.* (25), our data confirm the roles of calpain and caspase, respectively, in the dramatic fragmentation of Tau when cultured hippocampal neurons are treated with toxic levels of Aβ. We have expanded upon these earlier efforts by performing a detailed biochemical analysis of numerous key molecular events occurring either before or after Tau fragmentation. This includes both an examination of altered kinases as well as an extensive analysis of Aβ effects on Tau phosphorylation utilizing both site- and phospho-specific anti-Tau antibodies and one- and two-dimensional gels. These data demonstrate that proteolytic fragmentation of Tau followed by Tau fragment phosphorylation may be an important component of Aβ action in Alzheimer disease. Furthermore, our data are especially timely in view of a recent controversy regarding the toxic potential of the 17-kDa Tau fragment (17, 45). Our data indicate that the 17-kDa fragment alone is likely not sufficient to account for Aβ toxicity. Alternatively, we propose the combination of loss of full-length Tau together with the generation of multiple Tau fragments by both calpain- and caspase-mediated proteolysis converge to promote cell death after exposure to Aβ oligomers. Finally, the extensive analysis conducted in this study allows for a detailed chronological view of the many neuronal parameters affected by exposure to Aβ.

The most rapid events we observed upon Aβ treatment of the hippocampal neurons were induction of both calpain and caspase 3/7 activities. These findings are consistent with previous literature implicating caspase and calpain proteolysis as early events in the Alzheimer disease pathway (50, 51). Based on our protease inhibitor analysis, it appears that the early protease activities impact upon Tau function, degrading full-length Tau and creating low molecular weight Tau fragments. Indeed, calpain inhibition completely eliminated Aβ-mediated production of the 24-and 17-kDa Tau fragments, and caspase inhibition reduced the production of the 17-kDa fragment. These, and other Tau fragments have been implicated in neuronal dys-

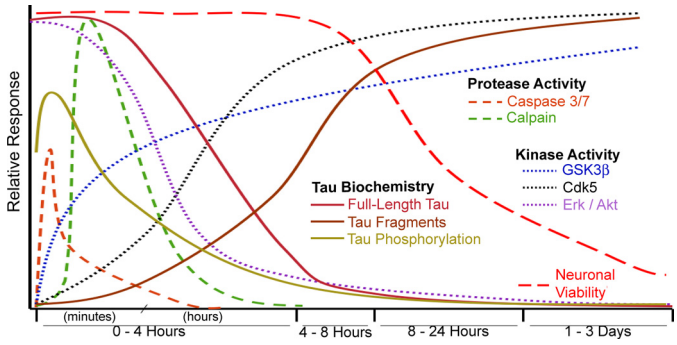

FIGURE 8. **Timeline summary of observed events on Aβ-treated hippocampal neurons.** The earliest events we observed were activation of caspase and calpain proteases, which display maximal activity within 20 min of Aβ treatment and return to normal levels by 4 h. Erk1/2 and Akt activities are depleted within 30 min to 1 h of Aβ treatment. GSK3β and Cdk5 activation also occurred rapidly and remained elevated throughout the entire time-course. These events precede and overlap with changes in Tau biochemistry, loss of full-length Tau, and accumulation of 17- and 24-kDa Tau fragments. The surprising lack of sustained Tau phosphorylation is depicted as an early spike (phosphorylated epitopes 181, 205, 262, and 400) and subsequent reduction. Events observed that are not depicted in this figure include reduced tubulin immunofluorescence between 8 and 24 h and the rapid and sustained increase in tubulin acetylation after Aβ treatment.

function and eventual cell death (17, 18). However, because our data demonstrate caspase and calpain inhibition protects against the production of Aβ-mediated low MW Tau fragments but only partially protect neuronal viability, it is likely that a combination of insults contribute to neuronal cell death (Fig. 5). It has recently been suggested that the 17-kDa Tau fragment is not toxic to neurons when overexpressed, in conflict with earlier data implicating the 17-kDa fragment as the source of Aβ-mediated toxicity (17, 45). Our results suggest the generation of this fragment likely contributes to toxicity but is not inherently toxic, as demonstrated by caspase inhibition dramatically reducing the production of this fragment but only providing mild protective effects in cell viability as measured by the ATP assay (Fig. 5).

How might one account for neuronal cell death that still occurs in the presence of both the calpain and caspase 3/7 inhibitors? Because both caspase and calpain inhibition failed to protect against the Aβ-mediated production of the slightly faster migrating Tau bands on SDS-PAGE, these may represent a Tau dysfunction independent of the proteases that contribute to neuron toxicity.

The lack of a dramatic effect of Aβ upon Tau phosphorylation is extremely surprising given the voluminous literature (46), especially as even our own data suggest GSK3β and Cdk5 activation. The Tau specificity of the site-specific antibodies we utilized was confirmed by their ability to recognize full-length Tau in wild type rat extracts and their failure to detect bands in the corresponding region of the gel from Tau knock-out mouse extracts (Fig. 5). The lack of dramatic Aβ-induced increases in Tau phosphorylation was independently confirmed by two-dimensional immunoblotting analysis, which would have easily detected significant changes in Tau phosphorylation via changes in Tau spot isoelectric points. Indeed, *in vitro* phosphorylation of Tau with purified Cdk5/p25 revealed the expected series of increasingly acidic spots on two-dimensional Tau immunoblots (data not shown). That our Aβ was biologically active was confirmed by its effects on kinase and protease activities and the ultimate induction of neuronal cell death. Thus, in our hands Aβ does not dramatically alter Tau phosphorylation as part of its promotion of neuronal cell death. Stated another way, marked Tau hyperphosphorylation is not necessary for Aβ/Tau-mediated neuronal cell death. However, we did observe rapid, transient, and relatively subtle increases in Tau phosphorylation at four sites. In principle, these phosphorylation events could be involved in initiating downstream biochemical events contributing to cell death. Interestingly, phosphorylation at one of these sites, serine 262, has been detected in "pre-tangle" neurons, suggesting this modification is an early disease-related event (52). Furthermore, Tau phosphorylated at serine 262 exhibits reduced ability to bind and polymerize microtubules (53), early events likely involved in the demise of neurons. A more detailed and focused analysis of these four specific sites will be required to elucidate their possible roles in promoting Aβ-mediated neuronal cell death. Finally, it is notable that every one of the 11 sites tested for phosphorylation exhibited reactivity with the phospho-specific antibodies even in healthy control cells that were not treated with Aβ and are readily detected with immunofluorescence microscopy in the neurites of healthy neurons (Fig. 6). This suggests that none of the sites tested here is inherently toxic when phosphorylated.

If Aβ does not induce dramatic Tau phosphorylation, how might one explain the vast literature showing Tau hyperphosphorylation in the Alzheimer brain? One possibility is that Tau hyperphosphorylation is indeed a key component of the Alzheimer pathway but is not induced by toxic levels of Aβ, at least not by itself. Genetic analyses demonstrate that mutations in the Aβ parent molecule, APP, cause early-onset Alzheimer disease (54). The sites of those APP mutations implicate proteolytic processing as a likely participant in the process, a conclusion that is greatly strengthened by disease-linked mutations in presenilin, one of the APP proteolytic enzymes. However, the proteolytic generation of Aβ also generates equal quantities of two other peptides, the amyloid intracellular domain (AICD) and the large extracellular APP domain. Both of these fragments have been shown to cause neuronal dysfunction and cell death independent of Aβ (55, 56). Our experimental system focuses only on the toxic Aβ component of this multifaceted disease-related situation. It is plausible that both Aβ accumulation and liberation of the extracellular and/or intracellular APP fragments converge in disease progression, and Tau hyperphosphorylation may be a consequence of one or both of these other important components.

In contrast, Aβ promoted rapid and complete degradation of full-length Tau within a few hours of treatment, generating a family of smaller, relatively stable fragments. Because the Tau fragments shift toward an acidic pI on two-dimensional gels, consistent with increased phosphorylation, it is likely that Tau is first fragmented by proteases and then phosphorylated by kinases. This raises the question of why the fragments were not detected by any of the 11 site- and phospho-specific antibodies. Previous work has suggested that Aβ-mediated fragmentation of Tau generates a relatively stable 17-kDa fragment, likely located on the amino half of the molecule (17), which is con-

sistent with our detection of this fragment with both Tau-1 and Tau-5 antibodies. However, only 4 of the 11 phospho-epitopes that we assayed lie within this region, specifically 181, 199/202, 205, and 217. Indeed, there are numerous additional potential phosphorylation sites in the amino half of Tau, and additional probing of these sites will help determine the nature of phosphorylation on the Tau fragments.

Because previous work demonstrates that Aβ-mediated neuronal cell death requires Tau (6, 7), how might Aβ promote Tau-mediated neuronal cell death? As noted above, our data do not support a role for Aβ-mediated full-length Tau hyperphosphorylation under toxic conditions. On the other hand, Aβ-mediated Tau fragmentation could cause neuronal death via a number of possible, non-mutually exclusive mechanisms. For example, Tau fragments might promote Tau aggregation, which could be inherently toxic, as has been suggested in previous cell culture studies (57). Alternatively, cell death could be caused by the loss of normal Tau activity leading to misregulation of microtubule dynamics and microtubule function (58, 59). This scenario could be mediated by several possible mechanisms, such as (i) the degradation of full-length Tau, (ii) sequestration of full-length Tau by Tau aggregates, or (iii) fragment induced disruption of Tau oligomerization, as recently suggested (60). Yet another possibility is that the process of proteolyzing an abundant protein such as Tau might saturate and overwhelm the proteasome machinery, leading to cell death. Finally, it also should be noted that combined calpain and caspase proteolysis might produce other phosphorylated Tau fragments from the carboxyl terminus of the molecule that were too small to detect on our gels. Such fragments could represent species of phosphorylated Tau prone to aggregation and resistant to turnover by cellular machinery.

In summary, the most important conclusions of this paper are that Aβ-mediated neuronal cell death involves rapid and complete Tau fragmentation but no dramatic effects upon full-length Tau hyperphosphorylation. If full-length Tau hyperphosphorylation is indeed a part of the biochemical pathway leading to neuronal cell death in Alzheimer and related dementias, our data indicate that toxic Aβ does not mediate this effect, at least not by itself. These observations will be important to consider in the design of future efforts targeted at developing of rational therapeutics for Alzheimer disease.

Acknowledgments—We are very grateful to Monte Radeke for superb instruction and guidance in two-dimensional gel fractionation, to Hana Dawson (Duke University) for providing Tau knockout mouse brain tissue, and to the Neuroscience Research Institute/Molecular, Cellular, and Developmental Biology Microscopy Facility for training and access to instrumentation. We thank Andy Schumacher for in vitro Tau phosphorylation reactions and Chris Banna and Carolyn Radeke for assistance with cell culture procedures and advice on neuronal dissections. We also thank Andy Schumacher and Nikki LaPointe for superb comments on the manuscript and the members of the Feinstein laboratory for many helpful discussions. Finally, we thank Chris Banna, Thales Papagiannakopoulos, and Dave Buchholz for many interesting and enlightening discussions.

REFERENCES

1. Ballatore, C., Lee, V. M., and Trojanowski, J. Q. (2007) *Nat. Rev. Neurosci.* **8,** 663–672
2. Buée, L., and Delacourte, A. (1999) *Brain Pathol.* **9,** 681–693
3. Haass, C., and Selkoe, D. J. (2007) *Nat. Rev. Mol. Cell Biol.* **8,** 101–112
4. Beyreuther, K., Bush, A. I., Dyrks, T., Hilbich, C., König, G., Mönning, U., Multhaup, G., Prior, R., Rumble, B., Schubert, W., *et al.* (1991) *Ann. N.Y. Acad. Sci.* **640,** 129–139
5. Tanzi, R. E., and Bertram, L. (2005) *Cell* **120,** 545–555
6. Rapoport, M., Dawson, H. N., Binder, L. I., Vitek, M. P., and Ferreira, A. (2002) *Proc. Natl. Acad. Sci. U.S.A.* **99,** 6364–6369
7. Roberson, E. D., Scearce-Levie, K., Palop, J. J., Yan, F., Cheng, I. H., Wu, T., Gerstein, H., Yu, G. Q., and Mucke, L. (2007) *Science* **316,** 750–754
8. Hardy, J. A., and Higgins, G. A. (1992) *Science* **256,** 184–185
9. Selkoe, D. J. (1991) *Neuron.* **6,** 487–498
10. Walsh, D. M., and Selkoe, D. J. (2007) *J. Neurochem.* **101,** 1172–1184
11. Mi, K., and Johnson, G. V. (2006) *Curr. Alzheimer Res.* **3,** 449–463
12. Lai, R. Y., Gertz, H. N., Wischik, D. J., Xuereb, J. H., Mukaetova-Ladinska, E. B., Harrington, C. R., Edwards, P. C., Mena, R., Paykel, E. S., and Brayne, C. (1995) *Neurobiol. Aging* **16,** 433–445
13. Terwel, D., Muyllaert, D., Dewachter, I., Borghgraef, P., Croes, S., Devijver, H., and Van Leuven, F. (2008) *Am. J. Pathol.* **172,** 786–798
14. Hernandez, P., Lee, G., Sjoberg, M., and Maccioni, R. B. (2009) *J. Alzheimers Dis.* **16,** 149–156
15. Drechsel, D. N., Hyman, A. A., Cobb, M. H., and Kirschner, M. W. (1992) *Mol. Biol. Cell* **3,** 1141–1154
16. Jeganathan, S., Hascher, A., Chinnathambi, S., Biernat, J., Mandelkow, E. M., and Mandelkow, E. (2008) *J. Biol. Chem.* **283,** 32066–32076
17. Park, S. Y., and Ferreira, A. (2005) *J. Neurosci.* **25,** 5365–5375
18. Amadoro, G., Ciotti, M. T., Costanzi, M., Cestari, V., Calissano, P., and Canu, N. (2006) *Proc. Natl. Acad. Sci. U.S.A.* **103,** 2892–2897
19. Kayed, R., Head, E., Thompson, J. L., McIntire, T. M., Milton, S. C., Cotman, C. W., and Glabe, C. G. (2003) *Science* **300,** 486–489
20. Jan, A., Hartley, D. M., and Lashuel, H. A. (2010) *Nat. Protoc.* **5,** 1186–1209
21. Fedoroff, S., and Richardson, A. (2001) *Protocols for Neural Cell Culture*, 3rd ed., pp. 255–264, Humana Press, Totowa, NJ
22. Rothman, S. (1984) *J. Neurosci.* **4,** 1884–1891
23. Kosik, K. S., Orecchio, L. D., Bakalis, S., and Neve, R. L. (1989) *Neuron.* **2,** 1389–1397
24. Khurana, V., Lu, Y., Steinhilb, M. L., Oldham, S., Shulman, J. M., and Feany, M. B. (2006) *Curr. Biol.* **16,** 230–241
25. Gamblin, T. C., Chen, F., Zambrano, A., Abraha, A., Lagalwar, S., Guillozet, A. L., Lu, M., Fu, Y., Garcia-Sierra, F., LaPointe, N., Miller, R., Berry, R. W., Binder, L. I., and Cryns, V. L. (2003) *Proc. Natl. Acad. Sci. U.S.A.* **100,** 10032–10037
26. Bloom, G. S., Ren, K., and Glabe, C. G. (2005) *Biochim. Biophys. Acta* **1739,** 116–124
27. Nicholson, A. M., and Ferreira, A. (2009) *J. Neurosci.* **29,** 4640–4651
28. Shankar, G. M., Li, S., Mehta, T. H., Garcia-Munoz, A., Shepardson, N. E., Smith, I., Brett, F. M., Farrell, M. A., Rowan, M. J., Lemere, C. A., Regan, C. M., Walsh, D. M., Sabatini, B. L., and Selkoe, D. J. (2008) *Nat. Med.* **14,** 837–842
29. Ono, K., Condron, M. M., and Teplow, D. B. (2009) *Proc. Natl. Acad. Sci. U.S.A.* **106,** 14745–14750
30. Cheng, G., Yu, Z., Zhou, D., and Mattson, M. P. (2002) *Exp. Neurol.* **175,** 407–414
31. Townsend, M., Mehta, T., and Selkoe, D. J. (2007) *J. Biol. Chem.* **282,** 33305–33312
32. Song, L., De Sarno, P., and Jope, R. S. (2002) *J. Biol. Chem.* **277,** 44701–44708
33. Rankin, C. A., Sun, Q., and Gamblin, T. C. (2007) *Mol. Neurodegener.* **2,** 12
34. Cohen, P., and Frame, S. (2001) *Nat. Rev. Mol. Cell Biol.* **2,** 769–776
35. Hamdane, M., Sambo, A. V., Delobel, P., Bégard, S., Violleau, A., Delacourte, A., Bertrand, P., Benavides, J., and Buée, L. (2003) *J. Biol. Chem.* **278,** 34026–34034

36. Town, T., Zolton, J., Shaffner, R., Schnell, B., Crescentini, R., Wu, Y., Zeng, J., DelleDonne, A., Obregon, D., Tan, J., and Mullan, M. (2002) *J. Neurosci. Res.* **69,** 362–372
37. Patrick, G. N., Zukerberg, L., Nikolic, M., de la Monte, S., Dikkes, P., and Tsai, L. H. (1999) *Nature* **402,** 615–622
38. Lee, M. S., Kwon, Y. T., Li, M., Peng, J., Friedlander, R. M., and Tsai, L. H. (2000) *Nature* **405,** 360–364
39. Glantz, S. B., Cianci, C. D., Iyer, R., Pradhan, D., Wang, K. K., and Morrow, J. S. (2007) *Biochemistry* **46,** 502–513
40. Nath, R., Raser, K. J., Stafford, D., Hajimohammadreza, I., Posner, A., Allen, H., Talanian, R. V., Yuen, P., Gilbertsen, R. B., and Wang, K. K. (1996) *Biochem. J.* **319,** 683–690
41. Byun, Y., Chen, F., Chang, R., Trivedi, M., Green, K. J., and Cryns, V. L. (2001) *Cell Death Differ.* **8,** 443–450
42. Shimohama, S., Tanino, H., and Fujimoto, S. (1999) *Biochem. Biophys. Res. Commun.* **256,** 381–384
43. Tsuji, T., Shimohama, S., Kimura, J., and Shimizu, K. (1998) *Neurosci. Lett.* **248,** 109–112
44. Deleted in proof
45. Garg, S., Timm, T., Mandelkow, E. M., Mandelkow, E., and Wang, Y. (2011) *Neurobiol. Aging* **32,** 1–14
46. Johnson, G. V., and Stoothoff, W. H. (2004) *J. Cell Sci.* **117,** 5721–5729
47. Sudo, H., and Baas, P. W. (2010) *J. Neurosci.* **30,** 7215–7226
48. Janke, C., Holzer, M., Klose, J., and Arendt, T. (1996) *FEBS Lett.* **379,** 222–226
49. Sergeant, N., David, J. P., Goedert, M., Jakes, R., Vermersch, P., Buée, L., Lefranc, D., Wattez, A., and Delacourte, A. (1997) *J. Neurochem.* **69,** 834–844
50. Adamec, E., Mohan, P., Vonsattel, J. P., and Nixon, R. A. (2002) *Acta Neuropathol.* **104,** 92–104
51. Cribbs, D. H., Poon, W. W., Rissman, R. A., and Blurton-Jones, M. (2004) *Am. J. Pathol.* **165,** 353–355
52. Augustinack, J. C., Schneider, A., Mandelkow, E. M., and Hyman, B. T. (2002) *Acta Neuropathol.* **103,** 26–35
53. Biernat, J., Gustke, N., Drewes, G., Mandelkow, E. M., and Mandelkow, E. (1993) *Neuron* **11,** 153–163
54. Forman, M. S., Trojanowski, J. Q., and Lee, V. M. (2004) *Nat. Med.* **10,** 1055–1063
55. Ghosal, K., Vogt, D. L., Liang, M., Shen, Y., Lamb, B. T., and Pimplikar, S. W. (2009) *Proc. Natl. Acad. Sci. U.S.A.* **106,** 18367–18372
56. Nikolaev, A., McLaughlin, T., O'Leary, D. D., and Tessier-Lavigne, M. (2009) *Nature* **457,** 981–989
57. Khlistunova, I., Biernat, J., Wang, Y., Pickhardt, M., von Bergen, M., Gazova, Z., Mandelkow, E., and Mandelkow, E. M. (2006) *J. Biol. Chem.* **281,** 1205–1214
58. Bunker, J. M., Wilson, L., Jordan, M. A., and Feinstein, S. C. (2004) *Mol. Biol. Cell* **15,** 2720–2728
59. Feinstein, S. C., and Wilson, L. (2005) *Biochim. Biophys. Acta* **1739,** 268–279
60. Rosenberg, K. J., Ross, J. L., Feinstein, H. E., Feinstein, S. C., and Israelachvili, J. (2008) *Proc. Natl. Acad. Sci. U.S.A.* **105,** 7445–7450
61. Makrides, V., Shen, T. E., Bhatia, R., Smith, B. L., Thimm, J., Lal, R. and Feinstein, S. C. (2003) *J. Biol. Chem.* **278,** 33298–33304